

Wavelet-Based Extraction of Coherent Vortices from High Reynolds Number Homogeneous Isotropic Turbulence

Katsunori Yoshimatsu¹, Naoya Okamoto¹, Kai Schneider², Marie Farge³,
and Yukio Kaneda¹

¹ Department of Computational Science and Engineering, Graduate School of
Engineering, Nagoya University, Chikusa-ku, Nagoya 464-8603, Japan
yosimatu@fluid.cse.nagoya-u.ac.jp, okamoto@fluid.cse.nagoya-u.ac.jp,
kaneda@cse.nagoya-u.ac.jp

² MSNM-CNRS & CMI, Université de Provence, 39 rue Frédéric Joliot-Curie,
13453 Marseille Cedex 13, France
kschneid@cmi.univ-mrs.fr

³ LMD-IPSL-CNRS, Ecole Normale Supérieure, 24 rue Lhomond, 75231 Paris
Cedex 05, France
farge@lmd.ens.fr

Abstract. A wavelet-based method to extract coherent vortices is applied to data of three-dimensional incompressible homogeneous isotropic turbulence with the Taylor micro-scale Reynolds number 471 in order to examine contribution of the vortices to statistics on the turbulent flow. We observe a strong scale-by-scale correlation between the velocity field induced by them and the total velocity field over the scales retained by the data. We also find that the vortices almost preserve statistics of nonlinear interactions of the total flow over the inertial range.

Key words: wavelet, coherent vortices, high Reynolds number turbulence, energy transfer

1 Introduction

Wavelet techniques to analyze turbulence have been pioneered at the end of 1980ies [1, 2]. They have been developed and exploited to reveal nature of turbulence, to model it and to solve the Navier-Stokes equation directly in wavelet space [3, 4, 5, 6].

A wavelet-based coherent vortex extraction (CVE) method for two-dimensional flows have been introduced by the use of orthogonal wavelet decompositions [7]. This has been extended to three-dimensional flows [8, 9]. Coherent Vortex Simulation (CVS) proposed in [7] is based on deterministic simulation of the flow due to the coherent vortices by the use of an *adaptive* wavelet basis, while influence of incoherent background flow onto the coherent flow is

neglected or statistically modeled. CVSs of two-dimensional flows and three-dimensional turbulent mixing layers is presented in [10] and [11], respectively.

In this paper, the wavelet-based CVE algorithm is applied to data obtained by DNS of three-dimensional incompressible homogeneous isotropic turbulence at resolution 1024^3 which corresponds to the Taylor micro-scale Reynolds number of 471 performed on the Earth Simulator [12, 13]. We examine coherent contribution to statistics of the turbulent flow, especially the energy transfer, as part of a *prior* test on a CVS of three-dimensional high Reynolds number turbulent flow.

2 Wavelet Analysis and CVE

2.1 Vector Valued Orthogonal Wavelet Decomposition

We consider a vector field $\mathbf{v}(\mathbf{x}) = (v_1(\mathbf{x}), v_2(\mathbf{x}), v_3(\mathbf{x}))$ in $\mathbf{T}^3 = [0, 2\pi]^3$. Three-dimensional orthonormal wavelet analysis unfolds \mathbf{v} into scale, positions and directions using a mother wavelet Ψ_m constructed by tensor product of one-dimensional scaling function $\psi_0(x)$ and mother wavelet $\psi_1(x)$ as $\Psi_m(\mathbf{x}) = \psi_\xi(x_1)\psi_\eta(x_2)\psi_\zeta(x_3)$ ($\xi, \eta, \zeta = 0, 1$, and $m = \xi + 2\eta + 4\zeta$). We use the Coiflet 12, which is compactly supported, quasi-symmetric, defined with a filter of length 12, and has four vanishing moments. The field sampled on 2^J equidistant grid points in each space direction of the Cartesian coordinates can thus be decomposed into an orthogonal wavelet series:

$$\mathbf{v}(\mathbf{x}) = \bar{\mathbf{v}} + \sum_{\alpha=1}^J \mathbf{v}_\alpha(\mathbf{x}), \quad \text{and} \quad \mathbf{v}_\alpha(\mathbf{x}) = \sum_{\iota_1, \iota_2, \iota_3=0}^{2^{\alpha-1}-1} \mathcal{W}_{m, \boldsymbol{\iota}}^\alpha[\mathbf{v}] \Psi_{m, \boldsymbol{\iota}}^\alpha(\mathbf{x}), \quad (1)$$

where $\bar{\mathbf{v}} = \int_{\mathbf{T}} \mathbf{v}(\mathbf{x}) d\mathbf{x}/(2\pi)^3$, $\Psi_{m, \boldsymbol{\iota}}^\alpha(\mathbf{x}) = 2^{3\alpha/2} \Psi_m(2^\alpha \mathbf{x} - 2\pi \boldsymbol{\iota})$, $m = 1, 2, \dots, 7$ and $\boldsymbol{\iota} = (\iota_1, \iota_2, \iota_3)$. The l -th component of $\mathcal{W}_{m, \boldsymbol{\iota}}^\alpha[\mathbf{v}]$ is given by $\int_{\mathbf{T}} v_l(\mathbf{x}) \Psi_{m, \boldsymbol{\iota}}^\alpha(\mathbf{x}) d\mathbf{x}/(2\pi)^3$. The summation convention is used for repeated indices but not for the Greek indices. $\overline{\mathbf{v}_\alpha} = 0$ because $\overline{\Psi_{m, \boldsymbol{\iota}}^\alpha} = 0$. Readers interested in details on orthogonal wavelet transform may refer to, e.g. [2, 14].

2.2 CVE

A wavelet-based method to extract coherent vortices from two- and three-dimensional turbulent flows has been proposed [7, 8]. An orthogonal wavelet decomposition is applied to the vorticity field $\boldsymbol{\omega}$. A threshold based on denoising theory [15] splits the wavelet coefficients into two sets. The coherent vorticity $\boldsymbol{\omega}_C$ is reconstructed from few wavelet coefficients whose moduli are larger than a given threshold depending on the enstrophy and resolution of the field. After applying the method, we obtain two orthogonal fields: the coherent vorticity $\boldsymbol{\omega}_C$ and the incoherent vorticity $\boldsymbol{\omega}_I$. We also reconstruct the coherent and incoherent velocity fields induced by the coherent and incoherent vorticity fields, respectively. Readers interested in the details may refer to [7, 8, 9, 16, 17].

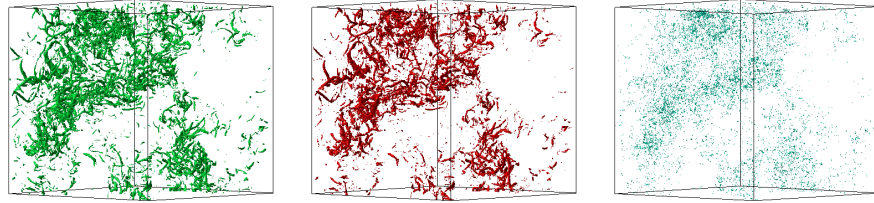


Fig. 1. Isosurfaces of total (left), coherent (middle) and incoherent (right) vorticity. The values of the isosurfaces are $|\boldsymbol{\omega}| = \omega_m + 3\sigma_\omega$ for the total and coherent vorticity and $2(\omega_m + 3\sigma_\omega)/5$ for the incoherent one. ω_m and σ_ω are the mean value of $|\boldsymbol{\omega}|$ and the standard deviation of $|\boldsymbol{\omega}|$, respectively. Subcubes of size 256^3 are visualized.

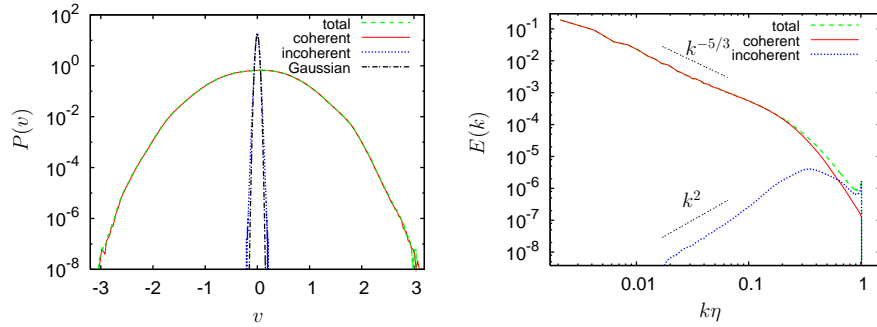


Fig. 2. Velocity PDFs (left) and energy spectra of the total, coherent and incoherent flow (right).

3 CVE from Homogeneous Isotropic Turbulence

We apply the CVE method to data obtained by DNS of three-dimensional homogeneous isotropic turbulence performed on the Earth Simulator [12, 13]. The DNS fields obey the Navier-Stokes equations for incompressible fluid in a periodic box with sides 2π . We use data for $k_{\max}\eta \simeq 1$ at resolution $N = 1024^3$ and the Taylor microscale Reynolds number $R_\lambda = 471$. Here k_{\max} is the maximum wavenumber retained in the DNS, and η is the Kolmogorov length scale.

We find that the coherent vortices are represented by the $2.9\%N$ wavelet coefficients of the total vorticity field. The flow induced by the vortices retains 99.7% of the energy and 81.0% of the enstrophy. Figure 1 shows that the coherent vorticity well retains the vortex tubes observed in the total vorticity. In contrast, we observe no vortex tube in the incoherent vorticity field.

The probability density functions (PDFs) and energy spectra of velocity of the total, coherent and incoherent flows are shown in Fig. 2 (left). All velocity PDFs exhibit quasi-Gaussian distributions. The total and coherent velocity PDFs well coincide, while the incoherent one has a strongly reduced variance.

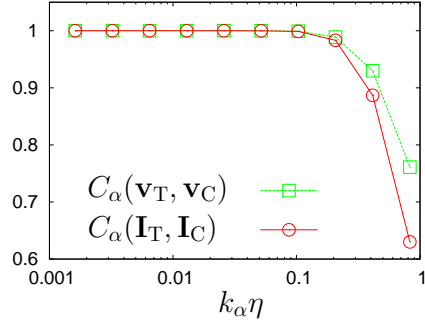


Fig. 3. $C_\alpha(\mathbf{v}_T, \mathbf{v}_C)$ and $C_\alpha(\mathbf{I}_T, \mathbf{I}_C)$ vs. $k_\alpha \eta$.

The spectrum of the coherent energy is identical to that of the total velocity all along the inertial range, presenting a $k^{-5/3}$ scaling, and that the spectrum of the coherent energy only differs from the one of the total energy in the dissipative range, where k is the wavenumber. For the incoherent velocity, we observe that $E(k)$ scales as k^2 , which corresponds to energy equipartition.

4 Contribution of Coherent Vortices to Energy Transfer

In order to examine contributions of the coherent vortices to energy transfer of the total flow, we consider scale-by-scale correlation between the vector fields due to the total flow and induced by the coherent vortices, and also the net energy transfer to scale α ($\alpha = 1, 2, \dots, \log_2 N^{1/3}$) at location indexed by ι proposed in [18].

The scale-by-scale correlation between vector fields $\mathbf{A}(\mathbf{x})$ and $\mathbf{B}(\mathbf{x})$ is defined by

$$C_\alpha(\mathbf{A}, \mathbf{B}) = \frac{\overline{\mathbf{A}_\alpha \cdot \mathbf{B}_\alpha}}{\sqrt{|\mathbf{A}_\alpha|^2} \sqrt{|\mathbf{B}_\alpha|^2}}. \quad (2)$$

Figure 3 shows the correlation $C_\alpha(\mathbf{v}_T, \mathbf{v}_C)$ and $C_\alpha(\mathbf{I}_T, \mathbf{I}_C)$ vs. $k_\alpha \eta$, where \mathbf{v}_T (\mathbf{v}_C) is the total (coherent) velocity field, $\mathbf{I}_\beta = (\mathbf{v}_\beta \cdot \nabla) \mathbf{v}_\beta + \nabla p_\beta / \rho$, $\beta \in (T, C)$, p_β the pressure obtained from $p_\beta = -\rho \nabla^{-2} [\nabla \cdot \{(\mathbf{v}_\beta \cdot \nabla) \mathbf{v}_\beta\}]$, ρ fluid density. $k_\alpha = 2^{\alpha-1} / 1.3$. $1/1.3$ for k_α is the centroid wavenumber of the Coifman 12. We find that the correlations are strong over all inertial scales. In the dissipative range, the latter is weaker than the former, and both of them decrease with increasing k_α .

The net energy transfer is given by $t_{\alpha, \beta}[\iota] = -\mathcal{W}_{m, \iota}^\alpha[\mathbf{v}_\beta] \cdot \mathcal{W}_{m, \iota}^\alpha[\mathbf{I}_\beta]$. Figure 4 shows mean and standard deviation wavelet spectra of the net energy transfers for the total and coherent flows. The spectra are normalized by $(\langle \epsilon \rangle \nu)^{3/4}$. Here $\langle \epsilon \rangle$ is the mean energy dissipation rate per unit mass of the total flow and ν is the kinematic viscosity. The mean wavelet spectrum $\tau_\beta(k_\alpha)$ is defined by $\tau_\beta(k_\alpha) = N_\alpha \langle t_{\alpha, \beta}[\iota] \rangle / \Delta k_\alpha$. Here, $N_\alpha = 2^{3(\alpha-1)}$ and

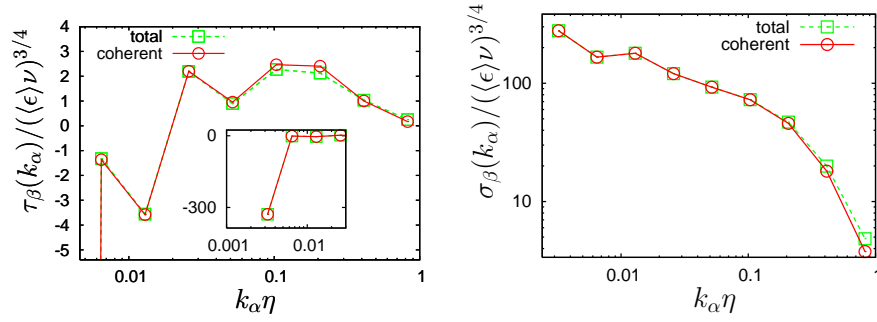


Fig. 4. Mean spectra (left) and standard deviation spectra (right) of the net energy transfer of the total and coherent flow. The standard deviation spectra are shown for $\alpha \geq 2$.

$\Delta k_\alpha = (k_{\alpha+1} - k_\alpha) \ln 2$. $\langle \cdot \rangle$ denotes the mean value of \cdot at each scale. The spatial variability of the energy transfer at each scale is measured by the standard deviation wavelet spectrum defined by

$$\sigma_\beta(k_\alpha) = N_\alpha \sqrt{\langle \{t_{\alpha,\beta}[\mathbf{t}]\}^2 \rangle - \langle t_{\alpha,\beta}[\mathbf{t}] \rangle^2} / \Delta k_\alpha. \quad (3)$$

In Fig. 4 we find that $\tau_C(k_\alpha)$ and $\sigma_C(k_\alpha)$ well coincides with $\tau_T(k_\alpha)$ and $\sigma_T(k_\alpha)$ in the inertial range, while, for $k\eta \gtrsim 0.1$, we observe a small discrepancy between $\tau_C(k_\alpha)$ ($\sigma_C(k_\alpha)$) and $\tau_T(k_\alpha)$ ($\sigma_T(k_\alpha)$).

5 Conclusions

The wavelet-based method to extract coherent vortices has been applied to the data of three-dimensional incompressible homogeneous isotropic turbulence at resolution 1024^3 grid points and $R_\lambda = 471$. The energy spectrum of the coherent flow is in good agreement with that of the total flow all along the inertial range. We observe a strong scale-by-scale correlation between the velocity field induced by the coherent vortices and the total velocity field at all scales. The statistics of nonlinear interactions are almost preserved by the coherent flow all along the inertial range. The present results encourage further development of the CVS of high Reynolds number turbulent flows. Dependence of contribution of coherent vortices to total fields on Reynolds number will be reported in another paper.

The computations were carried out on HPC2500 system at the Information Technology Center of Nagoya University. This work was supported by a Grant-in-Aid for the 21st Century COE ‘‘Frontiers of Computational Science’’, Grant-in-Aids for Scientific Research (B)17340117 from the Japan Society for the Promotion of Science and IPSL, Paris. We would like to express

their thanks to T. Ishihara, M. Yokokawa, K. Itakura and A. Uno for providing us with the DNS data. We also thank G. Pellegrino for providing his serial wavelet decomposition code (field16 written for a single processor) and T. Ishihara for support of the DNS data handling and for providing a FFT code that he parallelized in collaboration with T. Aoyama and M. Osada.

References

1. Farge M (1989) *J Fluid Mech* 206:433-462
2. Farge M (1992) *Ann Rev Fluid Mech* 24:395-457
3. van den Berg JC (Ed.) (1999) *Wavelets in Physics*. Cambridge University Press
4. Farge M, Schneider K (2002) *New Trends in Turbulence*. Les Houches 2000, Vol. 74 (Eds. Lesieur M, Yaglom A, David F), Springer: 449-503
5. Addison PS (2002) *The Illustrated Wavelet Transform Handbook*. Institute of Physics Publishing, Bristol and Philadelphia
6. Farge M, Schneider K (2006) In *Encyclopedia of Mathematical Physics* (Eds. Françoise JP, Naber G, Tsun TS), Elsevier:408-420
7. Farge M, Schneider K, Kevlahan N (1999) *Phys Fluids* 11:2187-2201
8. Farge M, Pellegrino G, Schneider K (2001) *Phys Rev Lett* 87:45011-45014
9. Farge M, Schneider K, Pellegrino G, Wray A, Rogallo B (2003) *Phys Fluids* 15: 2886-2896
10. Farge M, Schneider K (2001) *Flow Turb Comb* 66: 393-426
11. Schneider K, Farge M, Pellegrino G, Rogers M (2005) *J Fluid Mech* 534: 39-66
12. Yokokawa M, Itakura K, Uno A, Ishihara T, Kaneda Y (2002) *Proc IEEE/ACM SC2002 Conf*, Baltimore; <http://www.sc-2002.org/paperpdfs/pap.pap273.pdf>
13. Kaneda Y, Ishihara T, Yokokawa M, Itakura K, Uno A (2003) *Phys Fluids* 15:L21-L24
14. Mallat S (1998) *A Wavelet Tour of Signal Processing*. Academic Press
15. Donoho D, Johnstone I (1994) *Biometrika* 81:425-455
16. Schneider K, Farge M, Azzalini A, Ziuber J (2006) *J Turb* 7(44)
17. Azzalini A, Farge M, Schneider K (2005) *Appl Comput Harm Anal* 18: 177-185
18. Meneveau C (1991) *J Fluid Mech* 232:469-520